



HAL
open science

Impact of the GaN nanowire polarity on energy harvesting

Noelle Gogneau, Pascal Chrétien, Elisabeth Galopin, Stephane Guilet,
Laurent Travers, Jean-Christophe Harmand, Frédéric Houzé

► **To cite this version:**

Noelle Gogneau, Pascal Chrétien, Elisabeth Galopin, Stephane Guilet, Laurent Travers, et al.. Impact of the GaN nanowire polarity on energy harvesting. Applied Physics Letters, 2014, 104 (21), pp.213105. 10.1063/1.4880101 . hal-01096617

HAL Id: hal-01096617

<https://centralesupelec.hal.science/hal-01096617>

Submitted on 14 Oct 2022

HAL is a multi-disciplinary open access archive for the deposit and dissemination of scientific research documents, whether they are published or not. The documents may come from teaching and research institutions in France or abroad, or from public or private research centers.

L'archive ouverte pluridisciplinaire **HAL**, est destinée au dépôt et à la diffusion de documents scientifiques de niveau recherche, publiés ou non, émanant des établissements d'enseignement et de recherche français ou étrangers, des laboratoires publics ou privés.

Impact of the GaN nanowire polarity on energy harvesting

Cite as: Appl. Phys. Lett. **104**, 213105 (2014); <https://doi.org/10.1063/1.4880101>

Submitted: 11 March 2014 • Accepted: 14 May 2014 • Published Online: 29 May 2014

Noelle Gogneau, Pascal Chrétien, Elisabeth Galopin, et al.



View Online



Export Citation



CrossMark

ARTICLES YOU MAY BE INTERESTED IN

[Generation of electricity in GaN nanorods induced by piezoelectric effect](#)

Applied Physics Letters **90**, 063110 (2007); <https://doi.org/10.1063/1.2472539>

[Piezoelectric nanogenerator using CdS nanowires](#)

Applied Physics Letters **92**, 022105 (2008); <https://doi.org/10.1063/1.2831901>

[Effect of AlN buffer layer properties on the morphology and polarity of GaN nanowires grown by molecular beam epitaxy](#)

Journal of Applied Physics **110**, 053506 (2011); <https://doi.org/10.1063/1.3633522>



Trailblazers. New

Meet the Lock-in Amplifiers that measure microwaves.

Zurich Instruments [Find out more](#)

Impact of the GaN nanowire polarity on energy harvesting

Noelle Gogneau,^{1,a)} Pascal Chrétien,² Elisabeth Galopin,^{1,b)} Stephane Guilet,¹ Laurent Travers,¹ Jean-Christophe Harmand,¹ and Frédéric Houzé²

¹Laboratoire de Photonique et de Nanostructures, CNRS-LPN-UPR20, Route de Nozay, 91460 Marcoussis, France

²Laboratoire de Génie Electrique de Paris, UMR CNRS-Supélec 8507, Universités Pierre et Marie Curie et Paris-Sud, 11 rue Joliot-Curie, 91192 Gif sur Yvette, France

(Received 11 March 2014; accepted 14 May 2014; published online 29 May 2014)

We investigate the piezoelectric generation properties of GaN nanowires (NWs) by atomic force microscopy equipped with a Resiscope module for electrical measurements. By correlating the topography profile of the NWs with the recorded voltage peaks generated by these nanostructures in response to their deformation, we demonstrate the influence of their polarity on the rectifying behavior of the Schottky diode formed between the NWs and the electrode of measurement. These results establish that the piezo-generation mechanism crucially depends on the structural characteristics of the NWs. © 2014 AIP Publishing LLC. [<http://dx.doi.org/10.1063/1.4880101>]

Today it is highly desirable that nanodevices, such as sensors for environment monitoring, nomad electronics, or electronic board, operate without external batteries. To respond to this request, energy harvesting has received these last years a great attention. Among the alternative sustainable energy resources, the mechanical deformations and vibrations (such as body movements, sound vibrations, hydraulic movements, wind, and friction) present the advantages to be ubiquitous and available at all time. The piezoelectric nanowires (NWs) have emerged as excellent candidates to convert these types of energy into electrical energy. In fact, thanks to the superior mechanical properties (larger elasticity deformation, higher flexibility, and resistance),¹ higher sensitivity to applied force,^{1,2} and higher piezoelectricity properties^{3–5} in comparison with properties of the same material in bulk form, the NWs have the potential to fundamentally improve the electrical generator performance.

In 2006, the generation of electrical energy from the mechanical deformation of ZnO NWs has been demonstrated by Professor Wang from the Georgia Institute of Technology in USA.⁶ This concept has been also demonstrated for other piezoelectric 1D-nanostructures such as CdSe,⁷ CdS,⁸ PZT,⁹ and BaTiO₃.¹⁰ III-Nitrides nanostructures, despite their strong piezoelectric properties,^{5,11} have been much less studied. The first electric generation resulting from the deformation of GaN nanorod has been evidenced in 2007.¹² But it is only since 2010, that III-N NWs are investigated for the realization of generators. Among nitride materials investigated, we found NWs of GaN,^{13–15} AlN, and AlGaIn,¹⁶ and more recently InN.^{17,18}

In spite of the current research efforts on nanomaterials with the increased discussions on the benefits of nanowires to improve the energy conversion efficiency, there is a lack of fundamental understanding of piezoelectric properties of these nanostructures. This lack compromises the prediction of the piezoelectric potential, the improvement of the mechanical to electrical energy conversion, and thus the

development of optimized nanowire based piezo-generators. Only few studies have been reported on the properties of GaN NWs dealing with their piezoelectric generation capacity. Hence, it has been recently demonstrated that piezoelectricity in individual GaN NWs is six times stronger compared to bulk material⁵ and that the piezoelectric potential created inside the nanostructure is proportional to the NW deflection and saturates for the large deflections.¹⁴

In this Letter, we investigate the piezoelectric generation mechanism involved in bended GaN NWs by atomic force microscopy equipped with a Resiscope module for electrical measurements. We evidence the strong impact of the polarity of wurtzite NWs on their piezoelectric response. By correlating the topography profile of the deformed nanostructures with the recorded voltage peaks, we demonstrate the impact of the Nitrogen polarity of the GaN NWs on the rectifying behavior of the Schottky diode formed between the NWs and the electrode of measurement, the electric contact ensuring the charge recuperation for piezo-generation.¹⁹

GaN NWs were grown on Si(111) substrates in a plasma-assisted molecular beam epitaxy (PAMBE) chamber, active nitrogen being supplied by a radio-frequency plasma cell. The substrate temperature was fixed at 800 °C and the growth was performed under N-rich condition with an N/Ga ratio of about 1.36. Prior to the growth of GaN NWs, a 2.5-nm-thick AlN buffer layer was deposited on the substrate.²⁰ The GaN NWs formed under these conditions are vertically aligned NWs with hexagonal shape delimited by {10–10} planes²¹ (Fig. 1(a)). Due to the strong flexibility of GaN NWs and in order to finely characterize the piezoelectric properties of GaN NWs when they are deformed, we have partly encapsulated them into a thin polymethyl methacrylate (PMMA) layer in order to increase their mechanical resistance (Fig. 1(b)).¹³ Consequently, a higher deflection force could be used to improve the resolution and the reliability of the measurement. In these conditions, the emerging GaN NWs are characterized by a height of 121 ± 37 nm, a diameter of 88 ± 21 nm and a density of 3.8×10^{10} NW/cm².

One of the most common methods to measure the piezoelectric effect in NWs consists in involving lateral bending

^{a)} Author to whom correspondence should be addressed. Electronic mail: noelle.gogneau@lpn.cnrs.fr.

^{b)} Present address: Institute d'Electronique, de Microelectronique et de Nanotechnologie, Avenue Poincaré, 59652 Villeneuve d'Ascq, France.

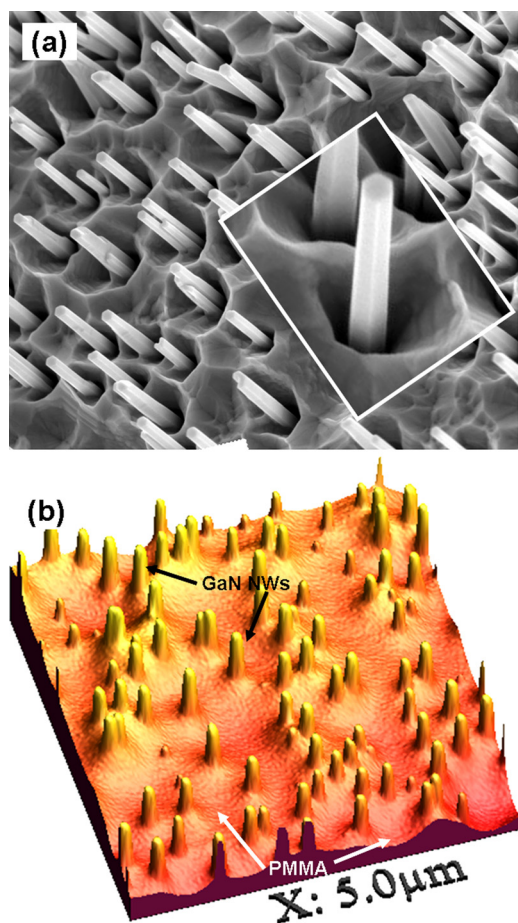


FIG. 1. (a) SEM image of GaN NWs grown by Plasma Assisted MBE; (b) 3D-topographic AFM image of partially encapsulated GaN NWs with PMMA.

of the nanostructure with simultaneous measurement of generated electric potential. This method requires a very sensitive measurement system, since the generated voltages and currents tend to be small when a single NW is tested. In this work, the electrical measurements were performed by an AFM in vertical configuration equipped with a modified Resiscope module.²² The AFM technique brings the advantage of the scanning and deflection measurements capabilities with a nanometer scale resolution. The Resiscope, which in its standard form allows dynamic resistance measurements over a very wide range (10^2 – 10^{12} Ω) in usual AFM scanning conditions, has been adapted in order to allow investigations on piezoelectric properties of NW samples similarly to the method used by Wang and coworkers.⁶ During scanning over the array of vertical NWs, the conductive AFM tip, which is brought into contact with the surface under a controlled and constant normal force, induces a local bending of the nanostructures. In response to this deflection and due to the piezoelectric effect, the NWs generate a voltage which is detected through the conductive AFM tip. In this measurement method, the external electrical is connected via an Ohmic contact formed between the NWs and the substrate, and a Schottky contact formed between the NW top and the AFM tip. In fact, concerning this last point, because we used a 30° cone-shaped doped-diamond tip characterized by a normal spring constant of 0.29 N/m, and because the electron affinity of the GaN is 4.1 eV and the work function of the doped-diamond is around 4.8 eV,²³ the diamond-GaN

contact forms a Schottky barrier which ensures the charge recuperation for piezo-generation.¹⁹ Throughout measurements, both the topographic and the electrical signals were recorded continuously and simultaneously. In our specific instrumental configuration, we do not apply any external voltage. The voltage waveform generated by the NW is observed across a load resistance R_L of 1 G Ω .

Figure 2 presents the AFM equipped with Resiscope module topographic image and the corresponding 3D images of output voltage peaks of the partially encapsulated GaN NWs recorded at a constant normal tip force of 173 nN. The output voltages measured are negative which indicate a n-type conductivity of our GaN NWs.²⁴ This experimental result is consistent with the n-type residual doping of GaN obtained with our growth conditions. GaN NWs generate an average output voltage about -74 mV, with the largest value reaching -443 mV. This latter value represents the highest output voltage reported for GaN-based NWs.¹³

In all the conductive AFM scans presented above, each voltage peak is correlated to the location of a nanowire. However, if we precisely analyze the correspondence between the topography profile of a given NW (Fig. 3(a)) and the corresponding voltage peak (Fig. 3(b)), we observe that the output signal is detected when the AFM tip gets in contact with the side of the n-doped GaN NW (Fig. 3(c)), i.e., when the deflection of the nanowires starts and the tip is in contact with the stretched side of the NW. The opposite behavior is observed with n-doped ZnO NWs: in this case, the output signal is generated when the tip is in contact with the compressed side of the NW.^{24–27} To understand this difference, we have to consider the piezoelectric properties of the constituting material. Due to the absence of inversion symmetry characterizing the wurtzite structures, the (0001)

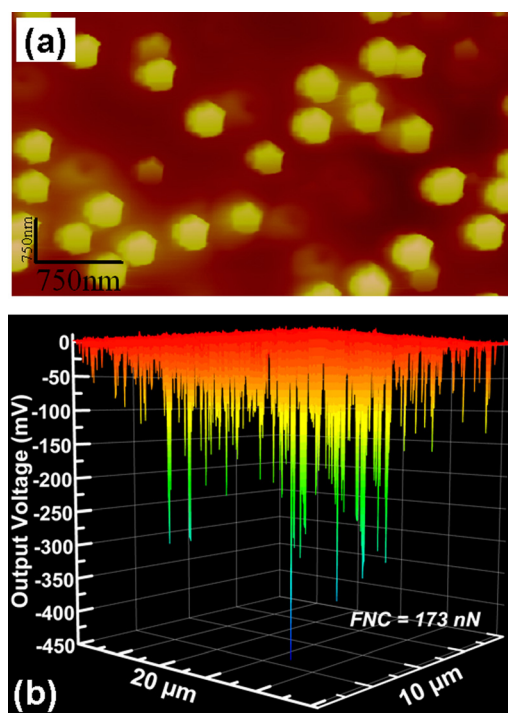


FIG. 2. (a) AFM equipped with Resiscope module topographic image and (b) corresponding 3D output voltages collected by AFM-Resiscope for a constant normal force of 173 nN.

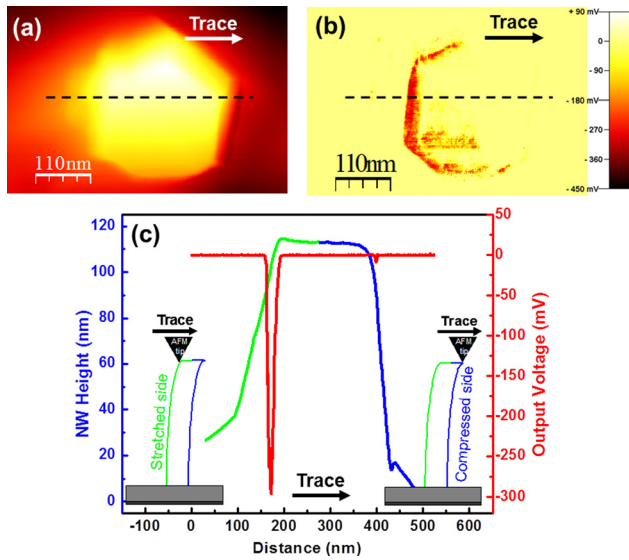


FIG. 3. Topographic (a) and output voltage (b) images of GaN NWs recorded by AFM-Resiscope for a normal constant force of 173 nN. The scanning direction is indicated by the arrows. (c) Corresponding topographic and electric profiles. The localization of the profile is materialized by the dashed line on Figs. (a) and (b). The output signal is detected only when the AFM tip starts to deflect the NWs, i.e., when the tip is in contact with the stretched side of the NW. We remark here that the NW diameter is higher than the one measured by SEM. This oversizing is attributed to the tip/surface convolution.

and (000 $\bar{1}$) surfaces of wurtzite III-nitrides, namely metal-face and N-face, respectively, are not equivalent. These two facets have different properties^{28–30} and the internal polarization along the z-axis of the NWs depends on the polarity of their top surface. We have previously shown that the GaN NWs synthesized under the growth conditions used for the present experiment, are terminated by an N-polar surface (N-polarity).²⁰ The spontaneous polarization (P_{SP}) is aligned with the z axis and oriented from N to Ga atoms. Thus, P_{SP} is parallel to the growth direction in our NW sample (Fig. 4(a)). However, this orientation plays a crucial role in the orientation of total polarization which includes the piezoelectric component created inside the nanostructures in response to an external applied force.

When the NW is laterally bended, an asymmetric strain is created across the NW. The outer face of the nanowire is stretched leading to a positive strain, while the inner face is compressed leading to a negative strain. As a consequence of this strain field, a piezoelectric polarization (P_{PZ}), which comes from a relative displacement of the Ga cations with respect to the N anions along the stress direction, appears inside the NW. Under compression, P_{PZ} is oriented anti-parallel to the spontaneous polarization and thus oriented opposite to the growth direction, while under stretching, P_{PZ} is parallel to the P_{PS} and aligned with the growth direction (Fig. 4(b)). A resulting piezoelectric field is created inside the NW volume. Due to the specific orientation of the piezoelectric polarization in the N-polar GaN NWs, the electric potential distribution evolves approximately between V_S^+ at the compressed facet and V_S^- at the stretched facet (Fig. 4(c)). Due to this electric potential variation through the NW volume, two different processes occur at the Schottky contact formed between the top of the n-type

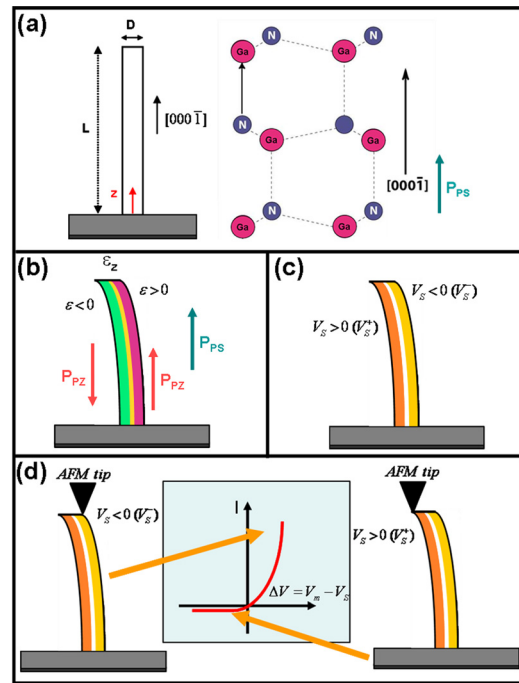


FIG. 4. (a) Representation of a NW and of the atomic arrangement of N-polar GaN structure. The spontaneous polarization is oriented from the nitrogen atoms towards the gallium atoms; (b) Strain distribution into the NW bent by conductive AFM tip; (c) Potential distribution into the NW; (d) Schottky contacts establish between the top of the NW and the conductive AFM tip for the stretched (right representation) and compressed (left representation) facets. These contacts lead, respectively, to a directly and a reversely biased Schottky diode.

doped GaN NWs and the conductive AFM tip (Fig. 4(d)). When the AFM tip starts to deflect the GaN NW, the contact between the tip and the stretched side is a positively biased Schottky diode ($\Delta V = V_m - V_S^- > 0$, where V_m is the potential of the metal tip, which is nearly zero). In consequence, charges flow across the interface driven by the piezoelectric potential. This results in an external output voltage detected across the load resistance. By contrast, when the conductive tip reaches the compressed face of the NW, the conductive AFM tip-GaN NW contact is a reversely biased Schottky diode ($\Delta V = V_m - V_S^+ < 0$) and there is no charge flow across the interface, explaining the absence of output voltage discharge.

By comparison, the n-type doped ZnO nanowires are characterized by the metal polarity, i.e., the NWs are terminated by Zn atoms.^{31,32} As for Ga-terminated GaN material, the metal-polarity of the ZnO NWs orients the P_{SP} in the (0001) direction (anti-parallel to the growth direction) (In wurtzite materials, the polarity is called metal-face when three of the bonds of the metal atoms with tetrahedral coordination face towards the substrate. By contrast, the polarity is called anion-face (N-face for GaN or O-face for ZnO) when three bonds face in the growth direction). The piezoelectric polarization in metal-polar structures is thus oriented in the opposite direction of the anion-polarity structures (N-terminated GaN or O-terminated ZnO). Consequently, the electric potential through the metal-polar ZnO NWs evolves between V_S^- at the compressed facet and V_S^+ at the stretched facet. This potential distribution explains the difference in the generation behavior between ZnO and our GaN nanowires. The different

Schottky diode behavior between the two materials is thus a direct consequence of the polarity of the wurtzite NWs. The understanding of this mechanism is essential to clarify the piezoelectric generation by NWs, to improve their energy conversion efficiency and to integrate them in adapted architecture of devices.

In summary, we have studied the piezo-generation properties of GaN NWs synthesized by PA-MBE. Under external mechanical solicitation of the nanostructures applied via an AFM system equipped with a Resiscope module for electric measurements, we have demonstrated that due to the N-polar character of the GaN NWs, the rectifying behavior of the Schottky contact created at the AFM-tip/NWs interface is inverted with respect to the n-type ZnO NW system. This behavior shows that the piezo-generation mechanism crucially depends on the structural characteristics of the NWs.

The improvement of the conversion efficiency and the prediction of the piezo-potential in 1D-nanostructures require a good knowledge of their structural and mechanical properties, but also a fine understanding of the strong role of the piezoelectric properties. To access at these properties, specific analyzes are necessary, notably by taking into account the impact of non-linear piezoelectricity in the strain nanostructures.^{33–35}

The authors thank J. Alvarez and L. Largeau for fruitful discussions.

¹X. Wang, *Nano Energy* **1**, 13 (2012).

²Y. S. Zhou, R. Hinchet, Y. Yang, G. Ardila, R. Sangmuang, F. Zhang, Y. Zhang, W. Han, K. Pradel, L. Montès *et al.*, *Adv. Mater.* **25**, 883 (2013).

³M. H. Zhao, Z. L. Wang, and S. X. Mao, *Nano Lett.* **4**, 587 (2004).

⁴R. Agrawal and H. D. Espinosa, *Nano Lett.* **11**, 786 (2011).

⁵M. Minary-Jolandan, R. A. Bernal, I. Kuljanishvili, V. Parpoil, and H. D. Espinosa, *Nano Lett.* **12**, 970 (2012).

⁶Z. L. Wang and J. H. Song, *Science* **312**, 242 (2006).

⁷Y. S. Zhou, W. Han, S. C. Rai, Y. Zhang, Y. Ding, C. Pan, F. Zhang, W. Zhou, and Z. L. Wang, *ACS Nano* **6**(7), 6478 (2012).

⁸Y. Lin, J. Song, Y. Ding, S.-Y. Lu, and Z. L. Wang, *Appl. Phys. Lett.* **92**, 022105 (2008).

⁹C. Y. Chen, T.-H. Liu, Y. Zhou, Y. Zhang, Y.-L. Chueh, Y.-H. Chu, J.-H. He, and Z. L. Wang, *Nano Energy* **1**, 424 (2012).

¹⁰Z. Wang, J. Hu, A. P. Suryavanshi, K. Yum, and M.-F. Yu, *Nano Lett.* **7**, 2966 (2007).

¹¹F. Bernardini, V. Fiorentini, and D. Vanderbilt, *Phys. Rev. B* **56**, R10024(R) (1997).

¹²W. S. Su, Y. F. Chen, C. L. Hsiao, and L. W. Tu, *Appl. Phys. Lett.* **90**, 063110 (2007).

¹³N. Gogneau, P. Chrétien, E. Galopin, S. Guilet, L. Travers, J.-C. Harmand, and F. Houzè, *Phys. Status Solidi RRL* **8**, 414 (2014).

¹⁴X. Xu, A. Potié, R. Songmuang, J. W. Lee, B. Bercu, T. Baron, B. Salem, and L. Montès, *Nanotechnology* **22**, 105704 (2011).

¹⁵C.-T. Huang, J. Song, W.-F. Lee, Y. Ding, Z. Gao, Y. Hao, L.-J. Chen, and Z. L. Wang, *J. Am. Chem. Soc.* **132**, 4766 (2010).

¹⁶X. Wang, J. Song, F. Zhang, C. He, Z. Hu, and Z. L. Wang, *Adv. Mater.* **22**, 2155 (2010).

¹⁷N.-J. Ku, J.-H. Huang, C.-H. Wang, H.-C. Fang, and C.-P. Liu, *Nano Lett.* **12**, 562 (2012).

¹⁸C.-T. Huang, J. Song, C.-M. Tsai, W.-F. Lee, D.-H. Lien, Z. Gao, Y. Hao, L.-J. Chen, and Z. L. Wang, *Adv. Mater.* **22**, 4008 (2010).

¹⁹J. Liu, P. Fei, J. Song, X. Wang, C. Lao, R. Tummala, and Z. L. Wang, *Nano Lett.* **8**, 328 (2008).

²⁰L. Largeau, E. Galopin, N. Gogneau, L. Travers, F. Glas, and J.-C. Harmand, *Cryst. Growth Des.* **12**, 2724 (2012).

²¹L. Largeau, D. L. Dheeraj, M. Tchernycheva, G. E. Cirlin, and J.-C. Harmand, *Nanotechnology* **19**(15), 155704 (2008).

²²O. Schneegans, P. Chrétien, and F. Houzè, French patent FR 10 01940, (5 May 2010), international PCT WO 2011/138738, (10 November 2011).

²³W. T. Zheng, C. Q. Sunb, and B. K. Tay, *Solid State Commun.* **128**, 381 (2003).

²⁴S. S. Lin, J. H. Song, Y. F. Lu, and Z. L. Wang, *Nanotechnology* **20**, 365703 (2009).

²⁵Y. Gao and Z. L. Wang, *Nano Lett.* **7**, 2499 (2007).

²⁶B. Perea-García, J. Zuniga-Perez, V. Munoz-Sanjose, J. Colchero, and E. Palacios-Lidon, *Nano Lett.* **7**, 1505 (2007).

²⁷Z. L. Wang, *Adv. Funct. Mater.* **18**, 3553 (2008).

²⁸R. M. Feenstra, J. E. Northrup, and J. Neugebauer, *MRS Internet J. Nitride Semicond. Res.* **7**, 3 (2002).

²⁹D. Huang, M. A. Reshchikov, P. Visconti, F. Yun, A. A. Baski, T. King, H. Morkoc, J. Jasinski, Z. Liliental-Weber, and C. W. Litton, *J. Vac. Sci. Technol. B* **20**, 2256 (2002).

³⁰H. W. Jang, J.-H. Lee, and J.-L. Lee, *Appl. Phys. Lett.* **80**, 3955 (2002).

³¹Z. L. Wang, *Mater. Today* **10**, 20 (2007).

³²Z. L. Wang, X. Y. Kong, and J. M. Zuo, *Phys. Rev. Lett.* **91**, 185502 (2003).

³³J. Pal, G. Tse, V. Haxha, M. A. Migliorato, and S. Tomić, *Phys. Rev B* **84**, 085211 (2011).

³⁴J. Pal, G. Tse, V. Haxha, M. A. Migliorato, and S. Tomić, *Opt. Quantum Electron.* **44**, 195 (2012).

³⁵J. Pal, M. A. Migliorato, Y.-R. Wu, B. G. Crutchley, I. P. Marko, and S. J. Sweeney, *J. Appl. Phys.* **114**, 073104 (2013).